COUNTING CHANNELS: A TUTORIAL GUIDE ON ION CHANNEL FLUCTUATION ANALYSIS

Osvaldo Alvarez,[1,2] Carlos Gonzalez,[1] and Ramon Latorre[1,2]

[1]*Centro de Estudios Científicos, Valdivia; and* [2]*Departamento de Biología, Facultad de Ciencias, Universidad de Chile, Santiago 6850240 Chile*

Ion channels open and close in a stochastic fashion, following the laws of probability. However, distinct from tossing a coin or a die, the probability of finding the channel closed or open is not a fixed number but can be modified (i.e., we can cheat) by some external stimulus, such as the voltage. Single-channel records can be obtained using the appropriate electrophysiological technique (e.g., patch clamp), and from these records the open probability and the channel conductance can be calculated. Gathering these parameters from a membrane containing many channels is not straightforward, as the macroscopic current $I = iNP_o$, where i is the single-channel current, N the number of channels, and P_o the probability of finding the channel open, cannot be split into its individual components. In this tutorial, using the probabilistic nature of ion channels, we discuss in detail how $i, N,$ and $P_{o\,max}$ (the maximum open probability) can be obtained using fluctuation (nonstationary noise) analysis (Sigworth FJ. *G Gen Physiol* 307: 97–129, 1980). We also analyze the sources of possible artifacts in the determination of i and N, such as channel rundown, inadequate filtering, and limited resolution of digital data acquisition by use of a simulation computer program (available at www.cecs.cl).

Ion channels are molecular machines, perfectly tuned to the transport of ions through the cell membrane, with very high efficiency (10^6-10^8 ions/s) [Latorre and Miller (13), Hille (11)]. Ion channels belong to a class of integral membrane proteins, some of which have evolved as highly selective to a given ion. For example, some potassium channels are ~1,000 times more permeable to K^+ than to Na^+. Amazingly, despite their exquisite ion selectivity, these channels do not lose their high ion throughput. Today, thanks to elucidation of the crystal structure of the K^+ channel from the bacterium *Streptomyces lividans* [Doyle et al. (5); Morais-Cabral et al. (14)], we understand how this high degree of ion selectivity is achieved. Channel opening and closing is a stochastic process. Transmembrane voltage determines the probability of finding the channels in either state, as in voltage-dependent channels, stretch in mechanosensitive channels, neurotransmitters in neurotransmitter receptor channels, or second messengers such as Ca^{2+} in Ca^{2+}-activated K^+ channels (11). Ion selectivity, ion conduction, and channel activation can be characterized using electrophysiological techniques such as patch clamping, which in its different modalities is used to determine single-channel properties [Neher and Sackmann (15), Sackmann and Neher (18)] and

voltage clamping employed when the current induced by a channel population is measured [Hodgkin and Huxley (12)]. Single-channel recordings contain information about the channel conductance, the probability of finding the channel open, and the distribution of open and closed dwelling times. This information is also present in the macroscopic currents measured in an ensemble of many ion channels. However, the process of retrieving this information from macroscopic currents is not straightforward. In this paper, we describe a procedure to analyze the fluctuations (nonstationary noise) in membrane conductance caused by opening and closing of ion channels. Using this methodology, we can reveal the number of channels (N) present in a membrane preparation, the unitary current (i) carried by a single channel, and the maximum probability of finding the channel open ($P_{o\ max}$). This tutorial is aimed at helping graduate students with solid knowledge of electrophysiology to search for these parameters from macroscopic current records when the need arises. We discuss the theory underlying this procedure and some of its limitations, and we present a step-by-step description of the method with examples generated using a computer program simulation. Sigworth (20) developed the nonstationary noise analysis to study Na^+ channels. The analysis is simple and powerful and much more comprehensible than those that use correlation functions or spectral densities.

We decided to write this tutorial because the apprentice biophysicist usually approaches membrane noise with apprehension, and we thought it convenient to give the interested scientist a friendly approach with emphasis on the concepts rather than the mathematics of the problem. Moreover, as stated in the preface of Louis de Felice's book (4) " . . . in the intervening years membrane noise became a definable subdivision of membrane biophysics."

This tutorial should be approached as an introductory lecture on noise analysis that should be complemented with the "hands-on" experience given by the educational computer program that we have developed, which is available at www.cecs.cl (1). Our experience has been that the tutorial is a good primer on the subject and can be handled independently by any Ph.D. student interested in the field and with some mathematics and physics background. Of course, the word "primer" should be taken in *sensum strictum*, and once the student is enticed by the subject, he/she should continue swimming in the rougher waters of the advanced approaches to noise analysis.

BASIC CONCEPTS

Classical experiments to characterize a voltage-dependent ion channel require measurement of current relaxation under voltage clamp. Membrane potential is depolarized for a short time, and the current is recorded. The current record contains information about both channel opening (during the depolarization) and channel closing (upon returning to the holding potential). A family of current records is usually studied using a series of stepped voltage pulses (Fig. 1*A*).

If we assume that the single-channel conductance is independent of the membrane potential, the following relation describes the measured current

$$I(t) = N\gamma P_o(V,t)(V - V_x) \qquad (1)$$

where $I(t)$ is the time-dependent ionic current experimentally observed; N is the number of channels in the preparation; γ is the single-channel conductance; $P_o(V,t)$ is the probability of finding the channel open, which is a function of time and membrane potential; V is the membrane potential, the variable controlled by the voltage-clamp system; and V_x is the reversal potential of the current. V_x is usually found using a double-pulse protocol. The prepulse (first pulse) opens the channels, and the test pulse (second pulse) closes the channels. The current measured during the test pulse is the tail current, which will be positive for V V_x or negative for $V < V_x$. In trials of many different test pulse voltages, a test pulse voltage will be found for which there is no tail current. This voltage is exactly V_x (Fig. 1*B*). A plot of I as a function of V crosses the current axis at $V = V_x$. The product $N\gamma P_o(V,t)$ is the slope of a cord drawn from V_x to a given point on the curve and is called the cord conductance.

Unless N and γ are known, the probability of finding the channel open cannot be determined from a simple analysis of current amplitudes. A classical current relaxation experiment on voltage-dependent channels consists of collecting membrane currents elicited
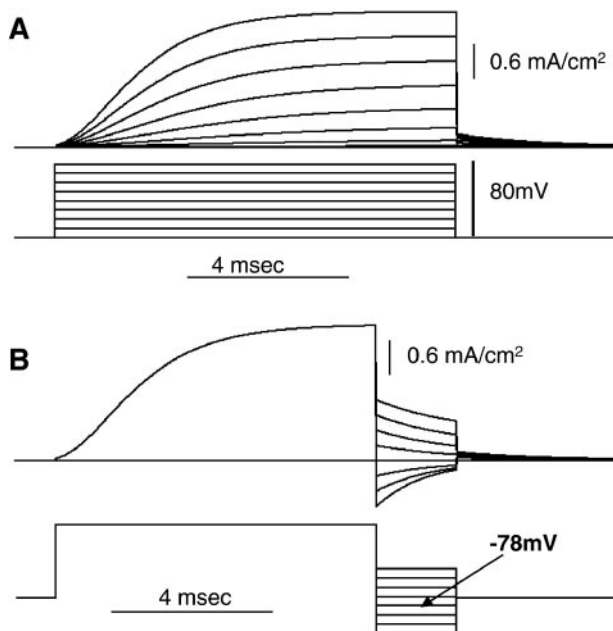
FIG. 1.

A: *top* traces are voltage-clamp macroscopic currents of squid axon K^+ channels during membrane depolarization. Holding potential is -67.1 mV. The membrane was successively depolarized in 10-mV steps, from 0 to 80 for 10 ms as shown in the *bottom* traces. B: double-pulse protocol used to obtain the reversal voltage (V_x). Channels were activated by an 80-mV voltage step from the resting potential of -67.1 mV followed by a series of 10-mV voltage steps to set the membrane potential between -106 and -36 mV. For these currents, the reversal potential is -78 mV, since there is no tail current at this membrane potential and the channels are open as can be seen when the voltage returns to the resting potential. Simulations were performed using "nerve" (3).

by a series of voltage pulses of increasing amplitude. Cord conductance, $I(t)/(V - V_x)$, is usually an S-shaped curve reaching an asymptotic value within the limit of very high voltages. Conductance as a function of voltage is customarily normalized as a fraction of this limiting value. According to *Eq. 1*, the maximum cord conductance is $N\gamma P_{o\,max}$, where $P_{o\,max}$ is the maximum open probability of the channel. $P_{o\,max}$ does not necessarily equal 1. One obvious mechanism producing a $P_{o\,max} < 1$ is channel inactivation, as found in classical sodium channels in nerve (20). A $P_{o\,max} < 1$ can also be found for a voltage-dependent channel in which the last step that opens the channel

is only weakly voltage dependent or is voltage independent. The product N multiplied by γ cannot be split into the individual terms N and γ in the classical analysis. Nonstationary noise analysis of the macroscopic current records provides tools to separate N from γ, and $P_{o\,max}$ can be determined as we describe below (20); for reviews see Heinemann (10), Heinemann and Conti (8), Neher and Stevens (16); for more details, De Felice (4) is recommended].

Single-channel noise. We consider a hypothetical ion channel with the following properties: *1*) the difference in current between closed and open states is directly proportional to membrane potential; *2*) the fraction of channels in the open state varies with membrane potential from 0 to 1 as the voltage increases; *3*) the statistics of the number of open channels in membranes with few channels follow a binomial distribution; and *4*) the voltage-dependent opening and closing of the channels explain the voltage-dependent properties of a membrane containing many channels. In other words, ion channels act independently of one another [e.g., Ehrenstein et al. (6)].

Figure 2 shows three representative records of a computer simulation of the time course of the current carried by this hypothetical ion channel at three different membrane potentials. Continuous records are split into 10 successive sections as shown. The straight horizontal line in each panel represents the average current recorded when the channel is closed. Channel opening appears as upswings of the current trace. Channels open and close randomly, and it is clear that the probability of finding the channel open is near 0 at 25 mV, about one-half at 45 mV, and close to 1 at 65 mV. There are two classes of current fluctuations (noise) visible in these records. The first class of noise appears as fluctuations of the trace around the closed channel current. These fluctuations are not related to membrane voltage-dependent properties and can be regarded as the equipment background noise.[1] The amplitude of this noise is the same for both an open and a closed channel. The second

---

[1] However, the current noise in an open channel can be much greater than the baseline noise. This can be caused by open and closed transitions too fast to be followed by the current-measuring system or by the shot noise induced by the statistical motion of ions as they flow through the open channel. These cases will not be
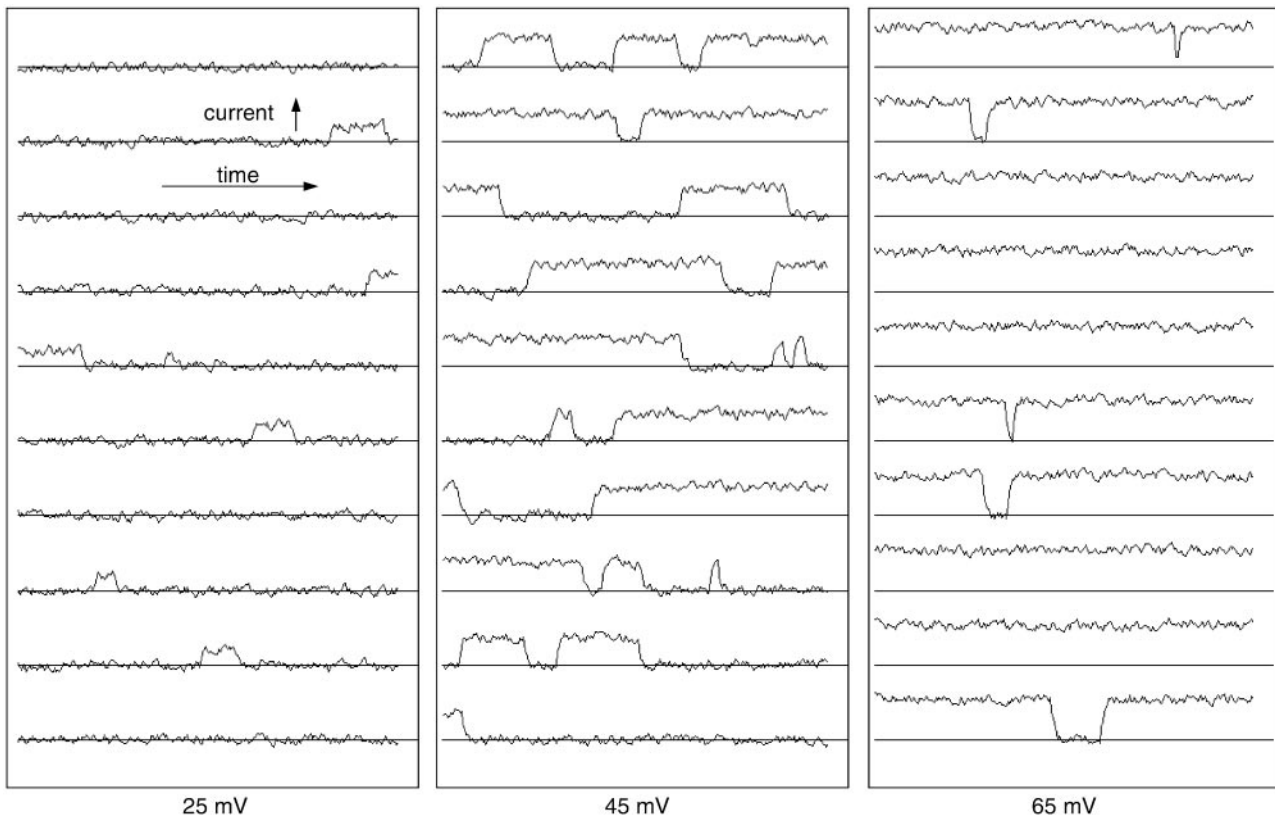
FIG. 2.

Single-channel recording simulations of a voltage-dependent channel. For each time step, a random number ranging between 0 and 1 is generated. If the random number is equal to or smaller than the transition probability, then the channel changes state or else remains in the same state. Simulation proceeds in small time steps to make sure that the probability of a transition for each time step is <1. The open-channel current is calculated as the product of the voltage and the single-channel conductance. Gaussian noise is added to all current values to simulate instrumental noise, and the current record is passed though a single-pole passive low-pass filter. Simulations are performed assuming a two-state channel where the kinetic constant α is the probability per unit time of the channel opening and β is the probability per unit time of the channel closing. Constants α and β are the voltage-dependent rate constants for each voltage, V, and are assigned these values: $\alpha = \alpha(0) \cdot \exp[2(V - 45)/25]$ and $\beta = \alpha(0) \cdot \exp[-2(V - 45)/25]$; $\alpha = \beta$ when $V = 45$ mV. The figure represents the time course of the current passing through a membrane with a single channel. Each panel has a continuous recording that has been cut into 10 successive sections for display. Horizontal line marks the baseline current of the closed channel. When the channel opens, current swings upward. Voltage units are mV; current and time units are arbitrary. Each upswing of the current is counted as an event.

class of noise is represented by the current trace that swings upward from the baseline every time the channel opens and that returns to the baseline when the channel closes. This is the noise that is directly related to channel opening and closing. Thus there is a noise impulse (or transition event) every time the channel

either opens or closes. The intensity of the noise can be evaluated by counting the number of current transitions observed during a period of time. In Fig. 2, we count 5 opening-closing events in the 25-mV record, where the channel is closed most of the time; 17 similar events in the 45-mV record, where the channel is open one-half of the time; and 5 events in the 65-mV record, where the channel is open most of the time. From this observation, we conclude that channel

---

discussed here, but the interested reader may consult Heinemann and Sigworth (9, 10).

noise depends on the probability of finding the channel open [$P_o(V,t)$]. The noise, or the number of transitions, is maximal when the probability of finding the channel open is 0.5, and this must be 0 when the channel is always closed or open. The probability of a transition occurring per unit time is proportional to the total number of channels. Therefore, it is clear that the noise level must depend on N, the number of channels present in the membrane.

Finally, noise must also depend on the amplitude of the unitary current fluctuation, $i = \gamma(V - V_x)$, which is the current carried by a single channel. The following section is the development of a theory that will be used to obtain $P(V,t)$, N, and i from the analysis of current fluctuations in membranes with a homogenous population of channels.

Mean current and variance. Let us consider a membrane with just one channel. Let us define p as the probability of finding the channel open and q the probability of finding the channel closed. Therefore

$$p + q = 1$$

The mean current $<I>$ passing through the single-channel membrane is the probability of finding the channel open multiplied by the single channel current i.

$$<I> = ip$$

The variance of the current, σ_I^2 is the sum of squared deviations from the mean, which can be calculated as the sum of each possible deviation multiplied by its probability.

$$\sigma_I^2 = q(0 - ip)^2 + p(i - ip)^2$$
$$= i^2(p^2q + pq^2) = i^2pq$$

In a membrane with N independent channels of the same kind, the mean current and the variance are N times larger than that of a single-channel membrane

$$<I> = Nip \tag{2}$$

$$\sigma^2 = Ni^2pq \tag{3}$$

Combining *Eqs. 2* and *3* gives the following expression

$$\sigma_I^2 = i<I> - \frac{<I>^2}{N} \tag{4}$$

Equation 4 is useful for understanding the relationship between noise due to channel gating and the fundamental channel characteristics. *Equation 4* is a parabola with roots on $<I> = 0$ and $<I> = iN$. There will thus be no noise when all of the channels are closed all of the time ($P_o = 0$) or when they are all open all of the time ($P_o = 1$). The first derivative of the function given in *Eq. 4* is

$$\frac{d\sigma_I^2}{d<I>} = i - \frac{2<I>}{N} \tag{5}$$

This derivative becomes zero for $<I> = iN/2$. Thus the variance has a maximum when the probability of finding the channel open is 0.5. *Equation 5* is the slope of the parabola, and within the limit of *very small* $<I>$ is the single-channel current i. When all of the channels are open, the mean current is iN; therefore, the slope is $-i$. In other words, the single-channel current can be obtained from the slope in the neighborhood of either root of the parabola.

This is the basis of the method used to calculate single-channel properties from the current fluctuation in a membrane containing many channels. We simply need to record steady-state current at a fixed potential and to compute the mean and the variance of the current. Once a strategy has been found to change the probability p to produce a well defined parabola, *Eqs. 4* and *5* can be used to compute the number of channels in the membrane, the unitary current, and the maximum probability of finding the channel open.

APPLYING THE METHOD TO VOLTAGE-DEPENDENT CHANNELS

An efficient strategy to determine the characteristics of voltage-dependent channels can be designed, since the probability of finding the channels open can be

readily altered. For instance, the P_o of K^+ channels in an excitable cell such as a neuron will be altered from 0 to $P_{o\ max}$ by changing the membrane potential from -70 mV to $+50$ mV. The change in P_o is not instantaneous, but it takes some time to change the open channel probability from zero to a constant steady value; P_o is a function of time and voltage. Figure 3 shows the result of 14 simulations of the current relaxation for an ensemble of 1,000 channels obtained using the simulation procedure that we released on www.cecs.cl. To compute the variance, the current relaxation experiment can be repeated M times, so there will be M measurements of I for each time point, i.e., for each value of the open-channel probability. The set of M points taken at any given time is called an isochrone (*iso* - 'equal', *chronos* - 'time'). All points on an isochrone have the same mean value of the open channel probability.

Figure 4 shows nine isochrones taken at different times for 100 current records similar to those of Fig. 3. Dispersion around the mean value is clearly smaller for the lower and upper isochrones where the open-
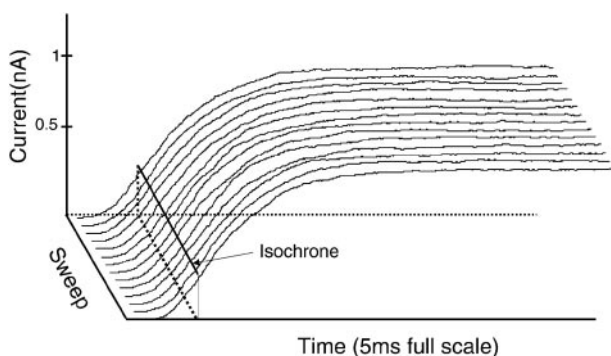

FIG. 4.
Nine isochrones taken at 9 different times. Each trace shows the instantaneous value of the current obtained at the same time after the start of each current relaxation for 100 successive time sweeps, similar to those shown in Fig. 3. Note that the dispersion of the current is small for the extreme values of the current, 0.05 and 0.95 nA, and maximal for the traces taken ~0.5 nA. Each simulation consists of 1,000 isochrones.

FIG. 3.
Samples of macroscopic currents simulated for voltage-dependent channels with 4 closed states and 1 open state. The simulation procedure is similar to the one outlined for Fig. 2, but here the forward kinetic constants (closed to open) are 4α, 3α, 2α, and α, and backward constants are β, 2β, 3β, and 4β. All channels are closed at $t = 0$ and relax to an open probability near 1. Each of the simulation current records shown is the ensemble average of 1,000 channels with a single-channel current of 1 pA, so the plateau current is close to 1 nA. The collection of data points read at the same time after the beginning of the voltage pulse (solid line parallel to the sweep axis) constitutes an isochrone.
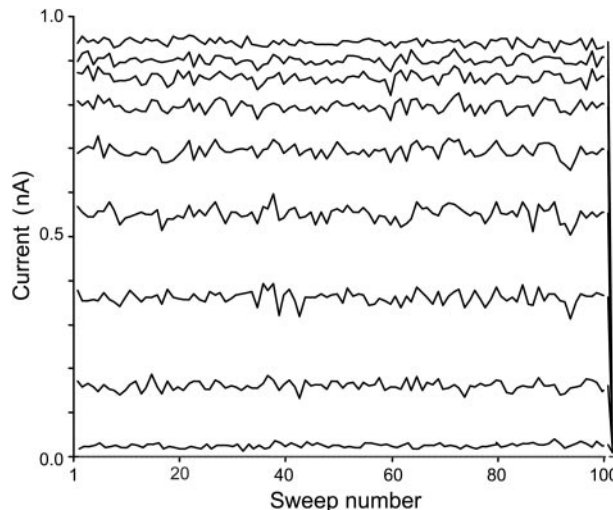
channel probability is near zero or near 1. It is maximal for the isochrone with a mean current of 0.5 nA, which corresponds to a 50% open probability. The mean current $<I>$ and its variance can be calculated for the points on each isochrone, as the expected probability of the open channel is the same for all the points on a given isochrone. The smooth line of Fig. 5 is a plot of the mean current of each of the 1,000 isochrones collected during the noise simulation as a function of the time after the start of the depolarization pulse at which the isochrone was measured. The jagged line is a plot of the variance of each isochrone as a function of time. The variance has a maximum value at a time at which the mean current is at one-half of its steady-state value. Figure 6 displays the variance as a function of the mean current for all of the 1,000 isochrones collected during the channel simulation. Parameters i and N can be obtained by nonlinear curve fitting using *Eq. 4*. The maximum open probability can be calculated from the maximum mean current recorded, $<I>_{max}$, divided by
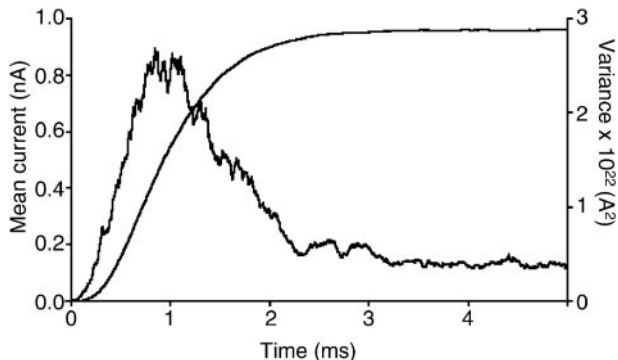
FIG. 5.

Plot of the mean current and variance as a function of time computed for each of the 1,000 isochrones collected during 20 successive depolarizations of a membrane with 1,000 channels. Unitary current was set to 1 pA, and the open probability (P_o) relaxed from 0 to 0.9. Note that the variance of the current is maximal at the time when the current is 50% of the steady-state current.

the mean current expected for a membrane with N open channels

$$P_{o\,max} = \frac{<I>_{max}}{iN} \qquad (6)$$

How the variance determination is affected by channel rundown. Under certain experimental conditions, the current recorded from a membrane may decrease unexpectedly during data collection; this problem is called channel rundown. A simulation of a membrane with channel rundown is shown in Fig. 7. In this simulated experiment, 200 sweeps were collected. The membrane contained 1,000 channels at the beginning of the experiment and only 800 at the end. Figure 7A shows selected isochrones. We can clearly see the scattering of the points along the isochrones and that it is clearly smaller for the lowermost and uppermost traces than for those obtained at relative currents between 0.3 and 0.8. However, this "bird's eye" appreciation of the noise structure in the isochrones is not consistent with the variance calculated using the standard formula as shown in Fig. 7B. Figure 7D is a closer display of an isochrone, and in Fig. 7E the deviations around the mean current are plotted. All deviations are positive for sweeps 1–100 and negative for sweeps 100–200. Because the dispersion is measured with respect to the mean of all

data points, the variance computed from these deviations will reflect mostly the rundown of the channels rather than the random variance of the number of open channels. A better method to calculate the variance relies on measurements of the differences in the current measured on successive sweeps. This method [Heinemann and Conti (8), Sigg et al. (19)] uses the differences (y_i) of successive points along the isochrone to calculate the variance, i.e.

$$y_i = \frac{1}{2}(x_i - x_{i+1}) \qquad (7)$$

where x_i is the ith point along the isochrone. By use of this transformation, the variance is now given by the expression

$$\sigma_I^2 = \frac{2}{N-1}\sum_1^N (y_i - \bar{y})^2 \qquad (8)$$

Figure 7F shows the deviations of the differences with respect to the mean of the differences y_i. Positive and negative deviations are evenly distributed and represent the random variations of the number of open channels. Figure 7C shows that the variance vs. mean current plot is now a parabola and that the values of
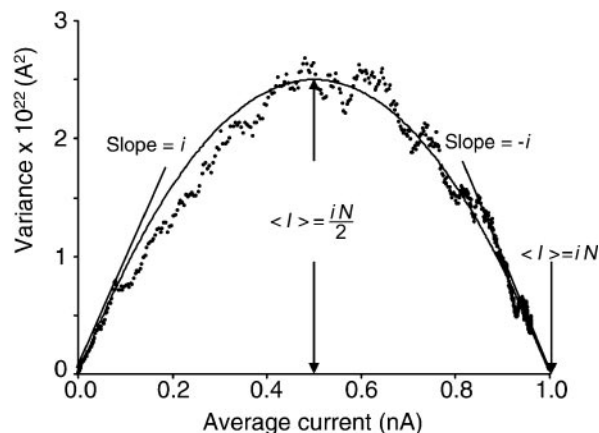

FIG. 6.

Plot of the variance vs. the mean current computed for each of the 1,000 isochrones of a simulation from data in Fig. 5. The slope of the curve at $I = 0$ is the single-channel current i. The positive intercept is i multiplied by N. The parabola was drawn according to *Eq. 4* with $i = 1$ pA, and $N = 1,000$.
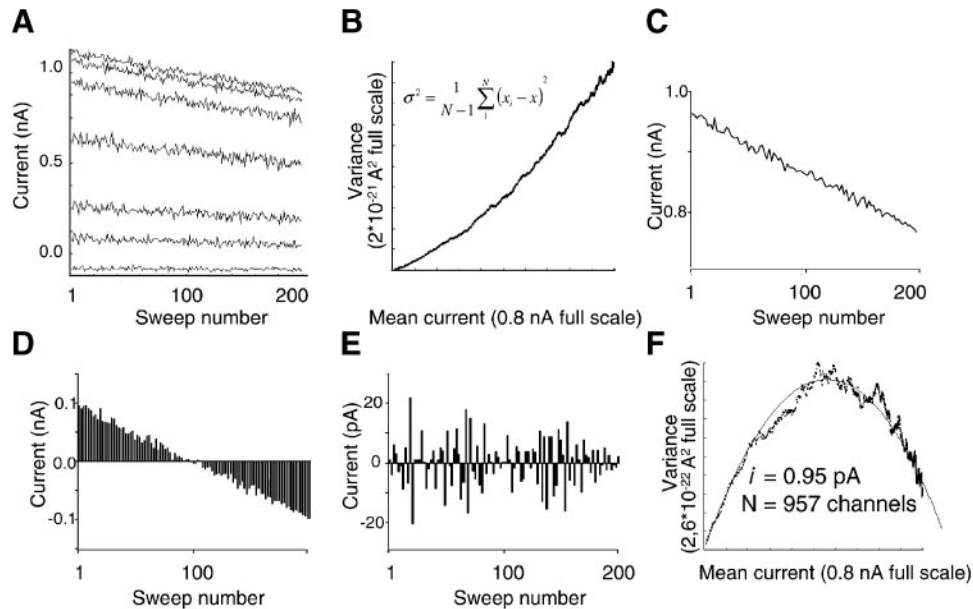
FIG. 7.

Mean-variance analysis in the presence of channel rundown. The membrane simulation initially had 1,000 channels with unitary current of 1 pA. Upon depolarization, the P_o relaxed from 0 to 0.9 following an exponential time course. The number of active channels decreases by 1 after each simulation of a depolarization, mimicking preparation rundown. We simulated the current of 200 depolarizations so that the membrane had 800 active channels on the last sweep. *A*: samples of isochrones showing the current rundown. *B*: variance vs. mean current plot of all 1,000 isochrones of the simulation. If data are not corrected for rundown, the variance grows indefinitely; this is because the current drift is proportional to the total current. Values for *i* and *N* cannot be retrieved from this analysis. *C*: a single isochrone displayed in an expanded scale. *D*: by use of the data in *D*, a bar plot of the deviations of the current of isochrone around the mean was constructed. *E*: bar plot of the differences between the current of successive sweeps corrected for the mean of the differences. The variance due to the random channel noise that is free from the artifact introduced by rundown can be calculated from these differences, and the result is shown in *F*. *F*: mean-variance plot obtained from the differences shown in *E* by use of the procedure of Heinemann and Conti (8), Sigg et al. (19), and Noceti et al. (17). The plot is now a parabola, and the correct values of *i* and *N* can be accurately retrieved.

i and *N* obtained from the fit to the data using *Eq. 8* are the expected ones.

How many channels in the membrane and how many repetitions are required for reliable measurements of *i* and *N*? In measuring macroscopic currents, we know that the relative current noise increases as the magnitude of the measured current decreases. Having large currents is thus convenient when the objective is a "clean" current record, but this can be a disadvantage when determining *i* and *N*

by use of noise analysis. This is because we are measuring the difference between the mean current and the current measured at a given time in the different current sweeps, and this difference, as we show below, will vanish as the $<I>$ becomes very large. Recalling *Eqs. 2* and *3*, and assuming that $P_o = 0.5$ for the sake of simplicity, we have

$$\frac{\sqrt{\sigma_I^2}}{<I>} = \frac{1}{\sqrt{N}}$$

This implies that, for a very large N, the standard deviation of I at any given time will be too small compared with $<I>$ to be measured accurately. This is especially important when using analog-to-digital conversion, since the minimum current difference that can be measured is one bit. In a 12-bit system, this is 1 part in 4,096. For example, let us consider a membrane with 10 channels, and we adjust our data acquisition system so the full amplitude of the macroscopic current is represented in 1,000 digital counts. Therefore, the unitary current is represented by 100 digital counts. To calculate the variance of the isochrones, we calculate the differences of the current recorded on successive sweeps. Figure 8A illustrates the differences recorded in the 10-channel membrane. The first six differences are 1, −1, 1, 0, 2, and −4 channels, which are accurately represented by 100, −100, 100, 0, 200 and −400 digital counts. Let us now consider a 10,000-channel membrane, in which we adjust the system so that the macroscopic current is represented again by 1,000 digital counts. In this case, each digital count will represent 10 channels. Figure 8B shows the current differences computed for this membrane, and we can see that all of the differences are multiples of 10 channels. This is an error introduced by the analog-to-digital conversion, since the actual differences are any integer number of channels. In this situation, our noise analysis will be inaccurate.

Our experience tells us that the accuracy of a determination depends on the size of the sample. This is also true for the mean-variance noise analysis. The accuracy of the determinations depends strongly on the number of sweeps collected during the experiments, i.e., the number of data points on each isochrone. As an example, we simulated the channel noise of a membrane with 1,000 channels and collected 100 sweeps. The standard deviation of a sample of 10 determinations was 20% of the central value for both the unitary current and the number of channels. Repeating the same procedure, but collecting 1,000 sweeps on each trial, reduced the standard deviation to 4%.

How reliable is the analysis when the experimental data cover only part of the parabola? Figure 9 shows a series of simulations in which the open-channel probability was explored to different
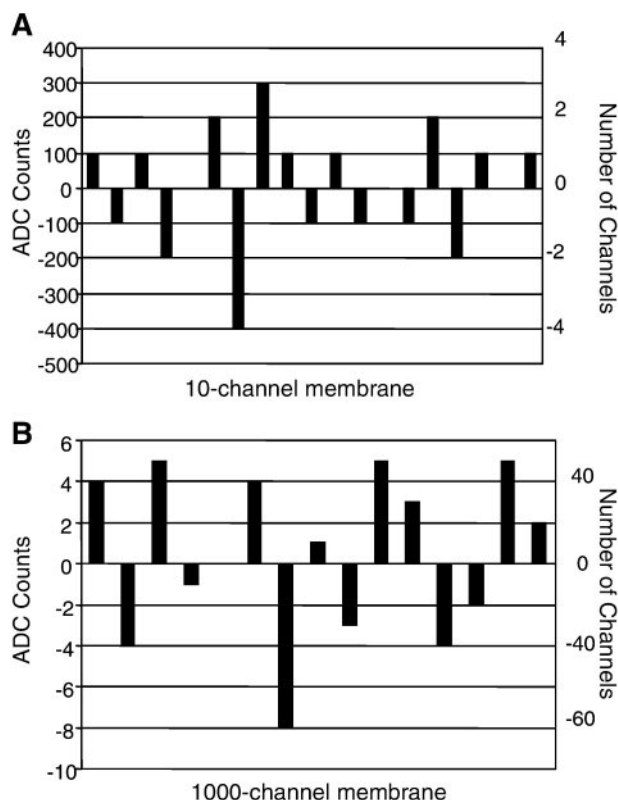

FIG. 8.
Current differences between successive isochrones. The analog signal was digitized using an analog-to-digital converter (ADC) that represents the full macroscopic current on 1,000 counts. *A*: current differences computed for a 10-channel membrane, where the current of a single channel is converted into 100 digital counts. In this case, the differences computed are accurate representations of the channel noise. *B*: differences computed in a 10,000-channel membrane, where each digital count represents 10 channels. In this case, the differences computed are a poor representation of the channel noise.

extents. Figure 9A represents the ideal case, where the open-channel probability changed from 0 to 1, and we thus have experimental points over the complete parabola. In Fig. 9B, the open-channel probability changed only from 0 to 0.1. In this case, the data look like a straight line rather than a parabola. In other words, only the slope of the variance-mean relation can be accurately calculated in this case. As mentioned earlier, the absolute value of the slope of the parabola near the roots is the unitary current i. Therefore, in this case, we can determine the unitary cur-
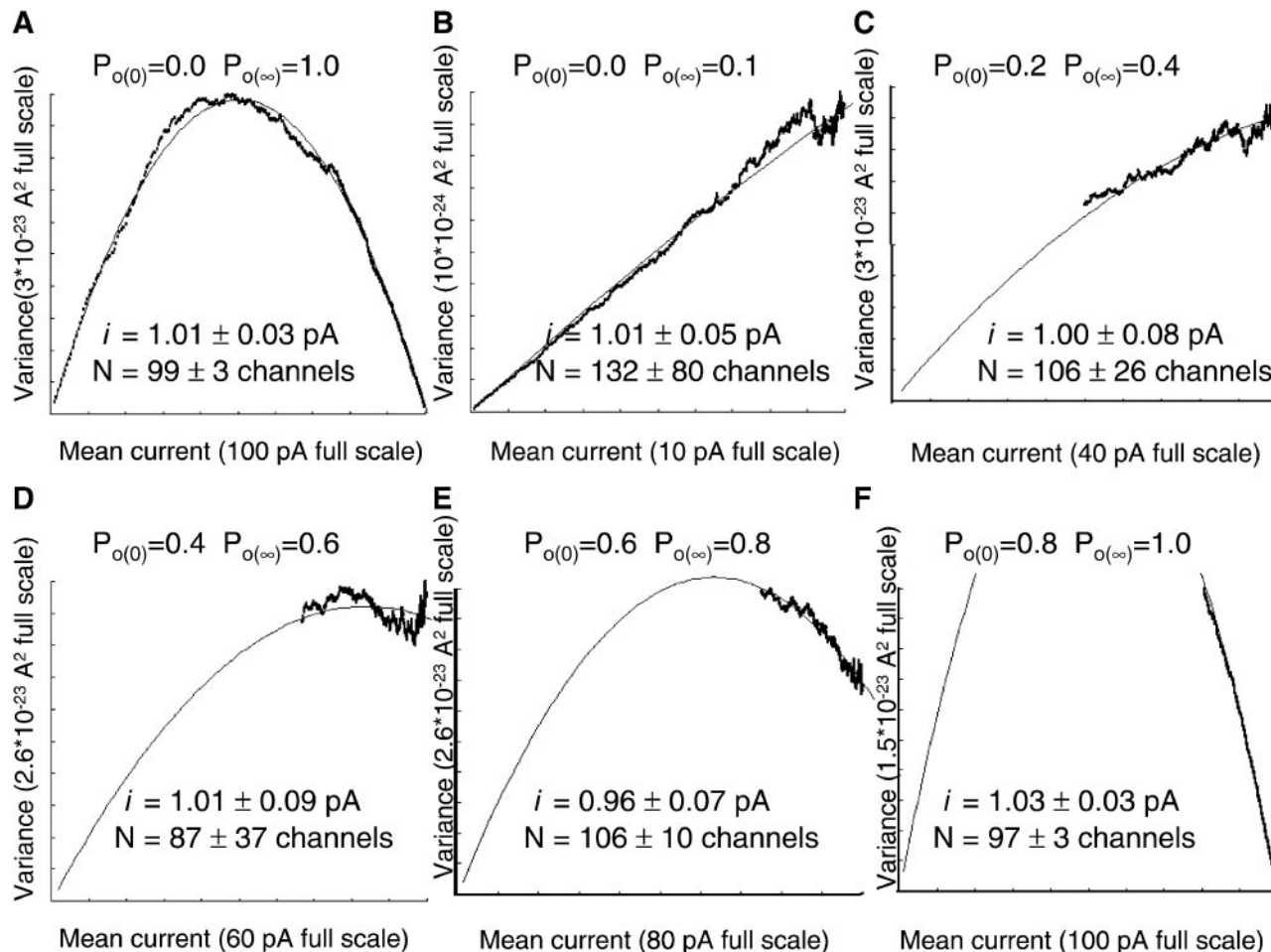
FIG. 9.

Exploration of the reliability of noise analysis under less than ideal conditions. Simulations were run setting the initial $P_{o(0)}$ and final $P_{o(\infty)}$ open-channel probability to different values as indicated at the top of each plot. The best least square parabola was fitted to the mean-variance experimental points computing single-channel current and the number of channels. Estimations of i and N were repeated 10 times for each experimental condition to compute a mean and a standard deviation of the sample, as shown under each curve. Note that the estimation of the single-channel current i is reliable for all cases shown here, *mirabile dictu*, even when the open time probability swings from 0.4 to 0.6. The number of channels in the membrane, N, is accurately determined only when data points are experimentally measured at an open-channel probability near 1.

rent but not the number of channels in the membrane. While producing the simulations for this tutorial, we were surprised to find that the unitary current can be estimated fairly accurately even for very limited explorations of the open probability space as shown in Fig. 9, *C, D,* and *E*. However, the number of active channels in the membrane, N, cannot be calculated accurately for situations where the complete parabola cannot be experimentally attained.

In Fig. 9*F*, we show a case in which the open-channel probability changed from 0.8 to 1. Despite the limited data points used to search for the best parabola, the fit gave accurate values for i and N (see Fig. 9*A*).

Figure 10 shows another situation where P_o never reaches 1.0 because of channel inactivation. In this case, the kinetic scheme has three states: closed, open, and inactivated, in which only the open state
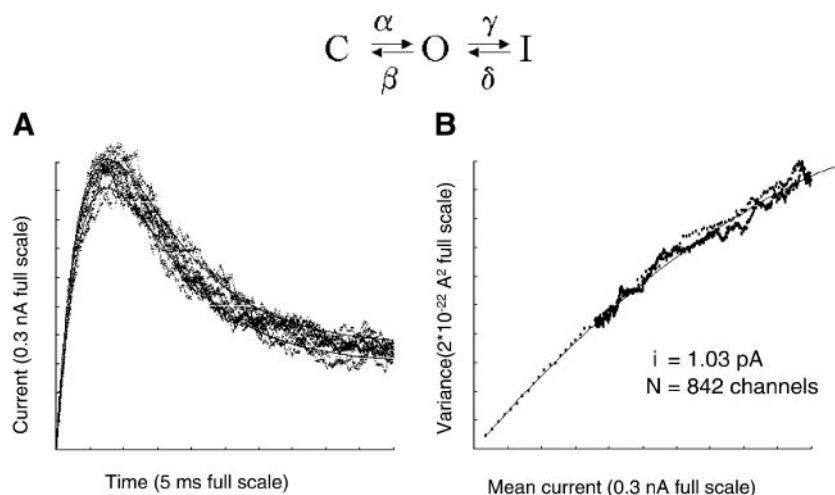
$$C \underset{\beta}{\overset{\alpha}{\rightleftharpoons}} O \underset{\delta}{\overset{\gamma}{\rightleftharpoons}} I$$

FIG. 10.

Noise analysis of channels that inactivate. Macroscopic currents were simulated for a membrane with 1,000 channels, with a unitary current of 1 pA for the open channel. Channel inactivation according to the kinetic scheme is shown in *A*, where state O carries current and states C and I are closed. *A*: superimposed image of 1,000 sweeps recorded. *B*: variance vs. mean current plot. Data points that appear separate, from low mean current to the maximum, correspond to the activation phase of the current. The points shown closer together correspond to the inactivation phase. All points are described well by the same parabola. Kinetic constants were $\alpha = 1,000$ s^{-1}, $\beta = 100$ s^{-1}, $\gamma = 2,000$ s^{-1}, and $\delta = 200$ s^{-1}.

carries current. Upon depolarization, channels are briefly in the open state and then proceed to the inactivated state. The time course of the current is represented in Fig. 10, in which the currents measured during several repeat experiments are superimposed. Current rises quickly and then decreases slowly to a steady-state value. The variance is plotted as a function of the mean current for each isochrone in Fig. 10*B*. It is clear from this figure that the data fit using *Eq. 4* effectively reproduces *i* but not *N* (actual number of channels is 1,000). It is interesting to note that time does not appear in the equation relating variance to the mean current. This means that the parabola can be drawn from $P_o = 0$ to $P_o = 1$ as well as from $P_o = 1$ to $P_o = 0$. This is why the sparse points belonging to the fast upstroke of the current as well as those closely spaced points belonging to the slower inactivation all fall on the same parabola.

Beware of the filter! It is our daily experience that passing the current record through a low-pass filter will reduce the noise. Thus we can anticipate that filtering will interfere with noise analysis. This is illustrated in Fig. 11, in which we filtered currents before performing noise analysis. The model we used is a two-state channel with a relaxation time of 1 ms. Filters with time constants of 0.3, 0.1, and 0.03 times the channel time constants were used. The distortion of the parabola and the errors in *i* and *N* are apparent when compared with the no-filter analysis. The lesson that we have drawn from of this example is that the filter must be set to a time constant well below those that describe channel gating. Because the rate of opening and closing of the channels may be unknown, demonstration of the stability of the results using different filters is mandatory.

The estimations of both *i* and the $P_{o\,max}$ can be seriously affected by choosing an incorrect filtering procedure, for example, in the case of a channel with a fast (flickering) between the open state and
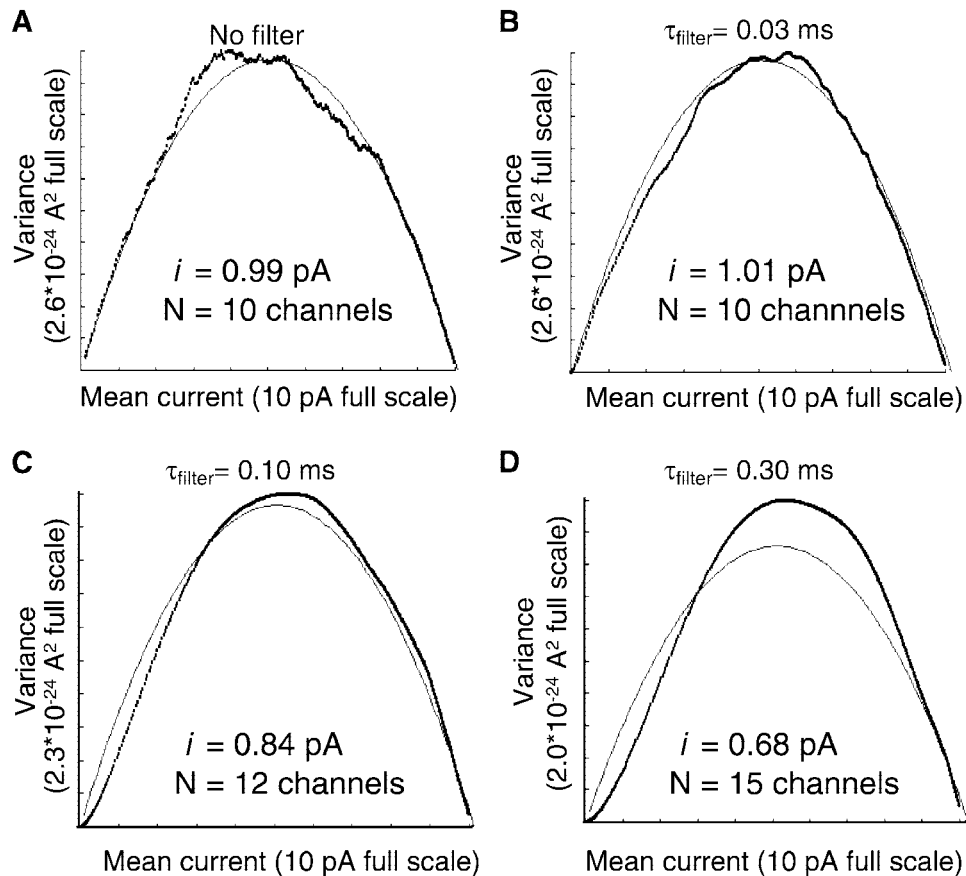
FIG. 11.

Noise analysis and low-pass filtering of the current signal. We simulated the relaxation of open-channel probability from 0 to 1.0 following an exponential time course with a time constant of 1 ms. Current records were filtered using an 8-pole Bessel low-pass filter. The −3-dB frequency of the filters used were 7,950, 1,590, and 795 Hz, corresponding to time constants of 0.03, 0.10, and 0.3 ms, respectively. τ_{filter} is the time constant indicated at the top of each plot. The retrieved values for unitary current and the number of channels are shown under each plot. The analysis yields correct results when the filter time constant is less than one-tenth of the channel relaxation time. Note the foot of the plot seen for low open-channel probability. This foot indicates that the single-channel current can no longer be calculated from the slope of the variance vs. mean current plot at low mean current (see Fig. 9B).

the closed state. The kinetic scheme of the simulation shown in Fig. 12 has two closed and one open state, C_1, C_2, and O. Exchange between the C_2 and O states is much faster than that between the C_1 and C_2 states. Upon depolarization, channels shift from state C_1 to C_2 and then reaches the state O. Figure 12A shows noise analysis performed in the absence of filtering. The analysis retrieves the cor-

rect values for i, N, and $P_{o\ max}$. Introducing a 10-kHz filter has the effect of halving i and increasing the $P_{o\ max}$ with almost no effect on the number of channels (Fig. 12B). The filter in this case eliminates the flicker collapsing the channel current, and since the filter eliminates the fast closing events the mean open time increases with consequent increase in $P_{o\ max}$.
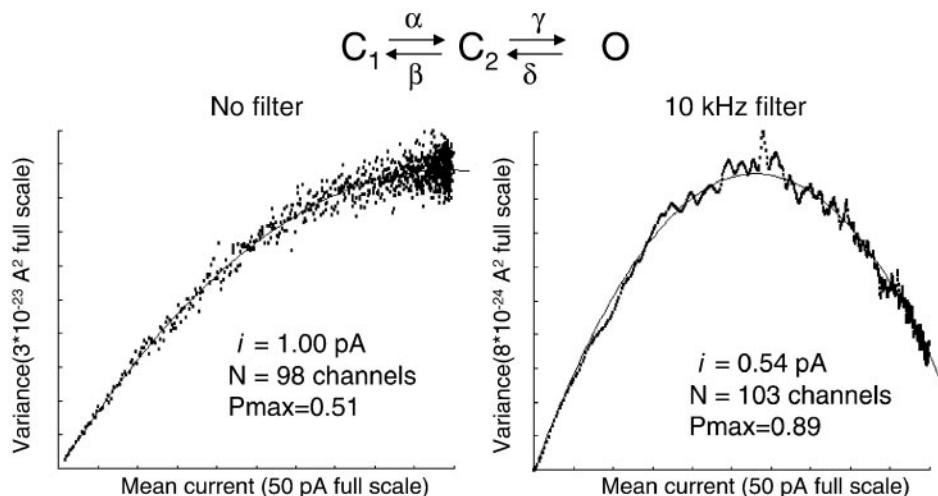
$$C_1 \underset{\beta}{\overset{\alpha}{\rightleftharpoons}} C_2 \underset{\delta}{\overset{\gamma}{\rightleftharpoons}} O$$

FIG. 12.

Flickering channels. This figure demonstrates the false results obtained for channels that flicker. To simulate these channels, we used the closed-closed-open scheme, as shown on *top*. Simulation begins with all channels in the closed state. After a first latency of 1 ms, channels enter a flickering state, opening and closing at a fast rate. The probabilities of finding the channel in the open or closed states are set to be equal, so the open probability in steady state is 0.5. The unitary current is 1 pA, and the number of channels (N) is 100. The simulation was run for 1,000 sweeps. *Left*: mean-variance plot in an ideal case where there is no filter. In this case, the analysis correctly retrieves i, N, and $P_{o\,max}$. *Right*: In this case, the current records are filtered using an 8-pole 10-kHz low-pass filter, the noise due to channel flicker is attenuated, and the analysis gives a false low unitary current and a false high maximum P_o (P_{max}, i.e., $P_{o\,max}$). Rate constants were $\alpha = 1$ ms^{-1}, $\beta = 0$, $\gamma = 100$ ms^{-1}, and $\delta = 100$ ms^{-1}.

NOISE ANALYSIS OF MACROSCOPIC CURRENTS OBTAINED USING THE PATCH-CLAMP TECHNIQUE

We close this tutorial by showing real data obtained using the patch clamp technique. The macroscopic current record shown in Fig. 13*A* is from a membrane macropatch in *Xenopus laevis* oocyte. In this case, the oocyte expressed calcium-activated K$^+$ channels (K$_{Ca}$, human *Slowpoke*). Using the same technique, we recorded outward currents flowing through *Shaker*H4Δ-(6–46) K$^+$ channels (Fig. 13*D*). Plots of variance vs. current corresponding to the raw data shown in Figs. 13, *B* and *E* and plots of variance vs. mean current are given in Figs. 13, *C* and *F*. The solid line is a fit to the data by using *Eq. 4*, yielding an estimate of the single-channel current, the number of channels contained in the patches, and the maximum probability of opening for K$_{Ca}$ and *Shaker* K$^+$ channels. These values can be converted to an estimate of the single-channel conductance dividing them by the driving force, which is 120 mV, because the internal and external K$^+$ concentration were the same. The values of single-channel conductances obtained for the K$_{Ca}$ and the *Shaker* channel were 175 pS and 12 pS, respectively. These values compare well with those measured directly from unitary currents.
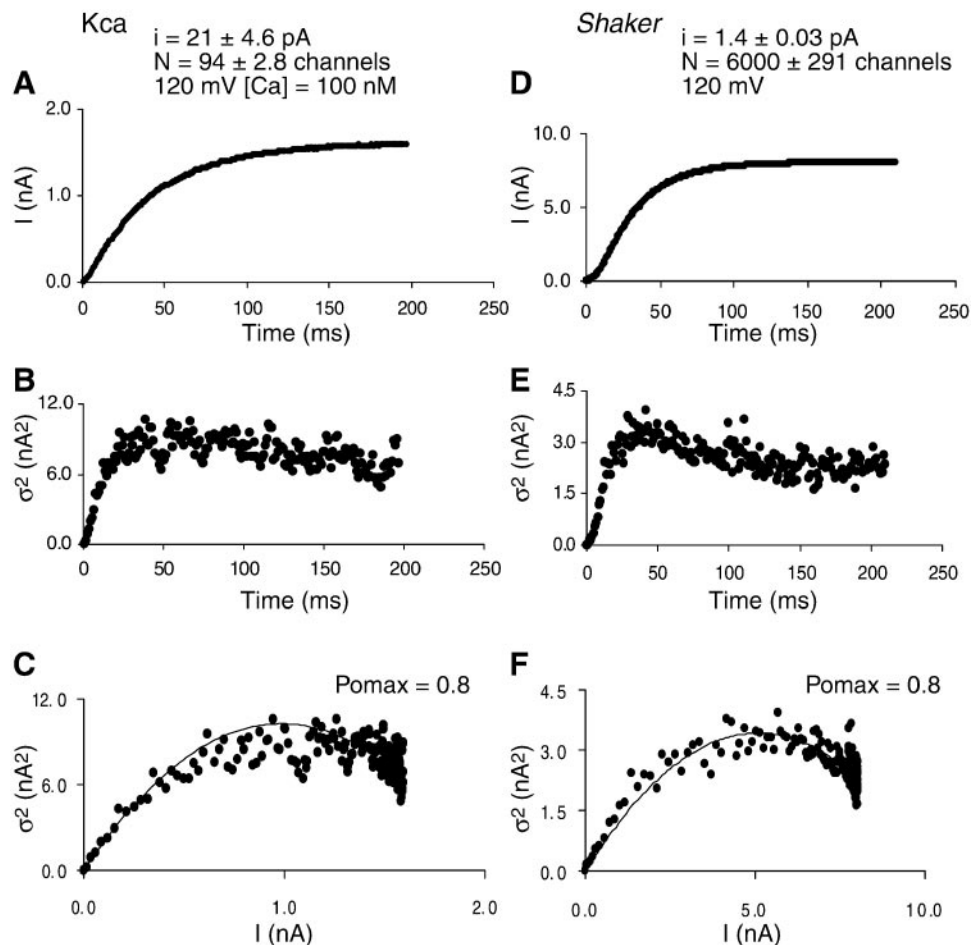
FIG. 13.

Nonstationary noise analysis of outward potassium currents flowing through calcium-activated K$^+$ channels (K$_{Ca}$) and *Shaker*H4Δ-(6–46). Channels were expressed in *Xenopus laevis* oocytes and detected using the macropatch technique. *A* and *D*: mean current traces obtained from 256 traces recorded with the patch technique from a holding potential of 0 mV (*A*, K$_{Ca}$ channel) or −100 mV [*D*, *Shaker*H4Δ-(6–46) channel] to a test pulse potential of 120 mV. In the case of the K$_{Ca}$ channel, the internal Ca^{2+} concentration was 100 nM. *B* and *E*: time course of the variance for the K$_{Ca}$ and the *Shaker*H4Δ-(6–46) channel, respectively. *C* and *F*: variance vs. mean current fitted to *Eq. 4* for the K$_{Ca}$ and the *Shaker*H4Δ-(6–46) channel, respectively.

Address for reprint requests and other correspondence: R. Latorre, Centro de Estudios Científicos, Avenida Arturo Prat 514, Valdivia, Chile (E-mail: ramon@cecs.cl).

REFERENCES

1. **Alvarez O, Gonzalez C, and Latorre R.** *Noise Simulation, a Teaching Computer Program*. www.cecs.cl.

2. **Begenisich T and Stevens CF.** How many conductance states do potassium channels have? *Biophys J* 15: 843–846, 1975.

3. **Bezanilla F.** *Electrophysiology and Molecular Basis of Excitability*. http://pb010.anes.ucla.edu/nervelt/nervelt.html.

4. **De Felice IJ.** *Introduction to Membrane Noise*. New York: Plenum, 1981.

5. **Doyle D, Morais-Cabral J, Pfuetzner R, Kuo A, Gulbis J, Cohen S, Chait B, and MacKinnon R.** The structure of the potassium channel: molecular basis of K+ conduction and selectivity. *Science* 280: 69–77, 1998.

6. **Ehrenstein G, Lecar H, and Nossal R.** The nature of the negative resistance in bimolecular lipid membranes containing excitability-inducing material. *J Gen Physiol* 55: 119–133, 1970.

7. **Heinemann SH.** Guide to data acquisition and analysis. In: *Single Channel Recording*, edited by Sackmann B and Neher E. New York: Plenum, 1995, p. 53–91.

8. **Heinemann SH and Conti F.** Nonstationary noise analysis and application to patch clamp recordings. *Methods Enzymol* 207: 131–148, 1992.

9. **Heinemann SH and Sigworth FJ.** Open channel noise. IV. Estimation of rapid kinetics of formamide block in gramicidin A channels. *Biophys J* 54: 757–764, 1988.

10. **Heinemann SH and Sigworth FJ.** Open channel noise. V. Fluctuating barriers to ion entry in gramicidin A channels. *Biophys J* 57: 499–514, 1990.

11. **Hille B.** *Ion Channels of Excitable Membranes.* Sunderland, MA: Sinauer Associates, 2001.

12. **Hodgkin AL and Huxley AF.** A quantitative description of membrane current and its application to conduction and excitation in nerve. *J Physiol* 117: 500–544, 1952.

13. **Latorre R and Miller C.** Conduction and selectivity in potassium channels. *J Membr Biol* 71: 11–30, 1983.

14. **Morais-Cabral JH, Zhou Y, and MacKinnon R.** Energetic optimization of ion conduction rate by the K^+ selectivity filter. *Nature* 414: 37–42, 2001.

15. **Neher E and Sakmann B.** Noise analysis of drug induced voltage clamp currents in denervated frog muscle fibres. *J Physiol* 258: 705–729, 1976.

16. **Neher E and Stevens CF.** Conductance fluctuations and ionic pores in membranes. *Annu Rev Biophys Bioeng* 6: 345–381, 1977.

17. **Noceti F, Baldelli P, Wei X, Qin N, Toro L, Birnbaumer L, and Stefani E.** Effective gating charges per channel in voltage-dependent K+ and Ca2+ channels. *J Gen Physiol* 108: 143–155, 1996.

18. **Sackmann B and Neher E.** The patch clamp technique. *Sci Am* 266: 44–51, 1992.

19. **Sigg D, Stefani E, and Bezanilla F.** Gating current noise produced by elementary transitions in Shaker potassium channels. *Science* 264: 578–582, 1994.

20. **Sigworth FJ.** The variance of sodium current fluctuations at the node of Ranvier. *J Gen Physiol* 307: 97–129, 1980.